

Ionization by early quasars and Cosmic Microwave Background anisotropies

N. Aghanim, F. X. Désert, J. L. Puget, and R. Gispert

IAS-CNRS, Université Paris XI, Batiment 121, F-91405 Orsay Cedex

Received date 4 April 1995 / accepted date 3 November 1995

Abstract. We discuss the photoionization of the intergalactic medium by early formed quasars and propose a mechanism which could generate measurable temperature fluctuations $\delta_T = \Delta T/T$ of the cosmic microwave background (CMB). Early quasars produce individual ionized regions around themselves. We evaluate both thermal and kinetic (first-order Doppler) Sunyaev-Zeldovich (SZ) effects associated with those ionized regions. Whereas the former is negligible, the latter induces the generation of detectable secondary small and medium scale CMB anisotropies. We find that this effect could produce measurable individual sources with a $\delta_T \simeq 10^{-6}$ to $\simeq 10^{-4}$ on scales up to 1° , which introduce a non gaussian signature in the statistics of the primordial anisotropies. The effect of the early formed quasars is compatible with the sources detected in Cheng et al. (1994) MSAM CMB experiment.

Key words: cosmology: cosmic microwave background – galaxies: quasars

1. Introduction

In most cosmological models, some reionization of the intergalactic medium (IGM) must have occurred between recombination and the present time where most of the gas is known to be already reionized (Gunn & Peterson 1965).

Several mechanisms were used to explain the ionization of the IGM. The possibility of photoionization has been extensively explored (Shapiro & Giroux 1987; Donahue & Shull 1987; Miralda-Escudé & Ostriker 1990; 1992). The possible sources of photons like young galaxies, primordial stars and decaying particles do not seem to be entirely satisfactory.

Apart from photoionization, the heating of the IGM may occur in some scenarios of galaxy formation involving explosions (Ikeuchi 1981; Vishniac & Ostriker 1985).

Send offprint requests to: N. Aghanim

Another possibility, which arises in hierarchical models, is ionization by high mass stars which form in subgalactic size clumps at high redshifts (Couchman & Rees 1986).

A detailed discussion of the various processes of reionization would be beyond the scope of this paper. We will focus our interest on the reionization by early quasars and how it affects the cosmic microwave background (CMB), knowing that Meiksin & Madau recently (1993) have shown that the quasars might indeed produce enough ionizing photons to completely ionize the IGM.

The main effect of the reionization is to wash out some of the temperature fluctuations of the CMB on small scales which undergo Thomson scattering on the reionized IGM (see for example Bond & Efstathiou 1984; Vittorio & Silk 1984; Tegmark et al. 1994).

In the assumption of a partial reionization by quasars, we present a new effect which, on the contrary, generates secondary small scale distortions on the CMB.

At times preceding the full reionization, quasars ionize the gas around themselves and they become surrounded by ionized bubbles. Those bubbles are moving together with the quasars in the large scale gravitational potential wells. Thus they have got a bulk peculiar velocity v , with respect to the local standard of rest in which the CMB is isotropic.

An effect equivalent to the Sunyaev-Zeldovich (SZ) kinetic effect for rich clusters creates relative temperature fluctuations which are proportional to the product of the Thomson optical depth τ by the ratio of the quasar radial velocity to the velocity of light (v_r/c) – between a line of sight crossing the ionized bubble and a nearby one which does not. Contrary to X-ray clusters, the corresponding thermal SZ effect, which is induced by the temperature of the gas is negligible in this case.

By comparison, the Vishniac effect (1987) induces distortions due to the correlations between the density and the velocity distributions in a *fully* ionized medium. The Vishniac effect is a second order one and it dominates on small angular scales (a few arcminutes or a few tens of arcminutes).

We investigate here a first order effect due to the bulk velocity of the ionized portion of the line of sight

Observing the primordial anisotropies of the CMB is the only way to constrain the various models of structure formation and give information about the origin of the fluctuations. In fact, the scale-invariant spectrum of mass density is preferred in many models. The standard picture of structure formation in an inflationary model naturally creates fluctuations with such a spectrum and a gaussian statistics. Cosmic defects, such as strings, textures..., are a different source of fluctuations. Although they might give a scale-invariant spectrum, they introduce a non-gaussian characteristic to the statistics of the fluctuations.

It is therefore important to determine whether or not the statistic of the observed primordial anisotropies is gaussian. In this context, it is thus also necessary to investigate mechanisms leading to deviations from gaussian statistics in the standard model. We find that the fluctuations induced by the early quasars are non-gaussian; this effect introduces a new component to the distortions and makes it harder to draw conclusions about the statistical nature of the primordial fluctuations.

Quasar formation theory is still in its infancy. Observations show the existence of quasars at redshifts as high as $z \approx 5$, although in hierarchical galaxy formation theories, the galaxies form late. We note that a recent work (Katz et al. 1994) shows that quasars could still be formed at high redshifts even in theories where galaxy formation occurs late such as in the hierarchical theories. The present work has no strong dependence on quasar formation theory, the presence of any high luminosity ionizing point sources will have the same kind of effect on the CMB, as long as it can roughly account for the reionization of the universe.

For the cosmological parameters, we used $h = H_0/100 \text{ km s}^{-1} \text{Mpc}^{-1} = 0.5$, $\Omega_0 = 1$ (flat universe) and $\Omega_b h^2 = 0.0135$ fraction of baryonic matter; according to the nucleosynthesis constraints we have $0.01 < \Omega_b h^2 < 0.015$ (Walker et al. 1991). Hereafter, we assume that there are no heavy elements other than those created in the Big Bang (H, D, He, Li, ...). Moreover, we neglect the contributions other than those induced by hydrogen and helium, and we assume that the quasars emit their radiation isotropically, producing spherical ionized bubbles. Possible geometrical effects were neglected in the present work. Owing to the high redshift range of interest, the hypothesis of homogeneity for the IGM gas is valid.

These approximations are justified in view of other uncertainties on the reionization process. The goal of this paper is to show that a non negligible effect is induced by this process and not to compute a detailed model.

In section 2 we discuss the relevant properties of an isolated bubble around a quasar and we compute the distortion of the CMB induced by such a bubble. In section 3 we compute the statistics over the whole sky of the distortions induced. In section 4 we present the results and discuss them in relation to recent CMB measurements.

2. Isolated early quasars and their effect on the CMB

The specific quasar model we use is a good illustration for effects induced by other possible sources of ionization like young ultraluminous galaxies for example.

We define the period of *isolated quasars* as the redshift range where most of the baryonic matter is still neutral while early quasars appear.

An isolated quasar emits strong radiation – in particular in the UV range – that can ionize the neutral intergalactic gas around it at great distance, thus creating an ionized sphere.

2.1. Ionizing radiation production rate

We first compute the size of the ionized sphere surrounding the quasar. Knowing the quasar specific luminosity in the B band, we deduce the emission rate S of UV photons ionizing the hydrogen atoms of the IGM.

The intrinsic spectrum of individual quasars in the ionizing UV domain is still uncertain but a good approximation is to use a power law extrapolation of the optical flux.

Several observations have been made in different spectral ranges (optical, X-rays ...) and constraint the values of the average spectral indexes in each range. A review of these observations was reported for example by Bechtold et al. (1987) who considered three spectral forms. We adopt the model consistent with the “medium” spectrum (Bechtold et al. 1987) which gives for the continuum spectral energy distribution radiated by quasars:

$$L_\alpha \propto \nu^{-1.5} \quad (\lambda < 1216 \text{ \AA}). \quad (1)$$

The luminosity function for quasars defined in Sect. 3.1 is written as a function of L_α the luminosity per spectral interval at the Lyman α frequency. It is therefore necessary to write S the UV emission rate – expressed in number of ionizing photons per unit time – as a function of L_α

$$S = \int_{\nu_{ion}}^{\infty} \frac{L_\alpha}{h_{pl}\nu} d\nu, \quad (2)$$

where h_{pl} is the Planck constant and ν_{ion} is the ionizing frequency for hydrogen.

Since the integral is dominated by the lower limit in frequency (ionizing limit for the hydrogen), the ionizing flux is not critically dependent on the assumed spectral shape. We get $S = AL_\alpha$ where A is a constant depending on the normalization of the spectrum. We introduce the following notation: a characteristic luminosity $L_\alpha^*(z_c) = L_c^*$ which is independent on the quasar age and will be introduced in Sect. 3.1, and defining the ratio $l_Q = L_\alpha/L_c^*$, one gets

$$S = \frac{L_c^*}{\alpha h_{pl}} \left(\frac{\lambda_{Ly}}{\lambda_{ion}} \right)^{-\alpha} l_Q. \quad (3)$$

$\alpha = 1.5$ is the spectral index of the quasar spectrum in the range of interest.

2.2. Temperature of the bubble

If the intergalactic matter around the quasar – essentially composed of hydrogen and helium – is ionized by the emitted radiation, the ionization of a hydrogen atom produces a photoelectron with an average kinetic energy defined by $\overline{E}_c = \overline{E}_{UV} - 13.6 \text{ eV}$, where \overline{E}_{UV} is the average energy of the ionizing photon.

Since electrons and protons rapidly thermalize owing to the short time scale of the Coulomb interactions, the electrons transfer about half of their energy to the protons, and the temperature of the plasma is thus given by $T = \overline{E}_c/3k_b$ as long as the cooling by recombination is negligible; here k_b is the Boltzmann constant.

We can compute the average energy of the ionizing photon $\overline{E}_{UV} = h_{pl}\overline{\nu}$ knowing the quasar spectrum and assuming that every photon is absorbed sooner or later:

$$\overline{\nu} = \frac{\int_{\nu_{ion}}^{+\infty} F_\nu d\nu}{\int_{\nu_{ion}}^{+\infty} \nu^{-1} F_\nu d\nu}. \quad (4)$$

We find $\overline{E}_{UV} \approx 40 \text{ eV}$, which leads to $T \approx 10^5 \text{ K}$ for the plasma temperature. A photoelectron even if it has an energy larger than 13.6 eV will have a very low probability to make a second ionization, the propagation of the ionization front being much faster than the electron velocity. Thus the number of ionization is very nearly equal to the number of ionizing photons. In that context, taking into account the presence of helium is equivalent to a 10% increase of the baryon density with hydrogen only. Therefore, in the following, we use $\Omega_b h^2 = 0.015$.

In the bubbles surrounding the quasars, the gas is fully ionized, therefore there is no cooling due to neutral atoms. The ionized gas will cool by bremsstrahlung (free-free radiation), but, the cooling time is longer than the age of the universe.

Likewise, we investigate the effect of the inverse Compton cooling and find that it will become important for redshifts greater than $10 h^{2/5}$ (cooling time equal to the age of the universe), or for $h = 0.5$, $z > 7.6$.

We check that the temperature of the bubble decreases by a factor 2 at $z = 10$, the Compton cooling does not change drastically the temperature. Since the exact temperature is not critical, we assume that it remains constant at $T \approx 10^5 \text{ K}$ but undergoes the adiabatic cooling due to expansion.

This approximation breaks down for redshifts significantly larger than 10.

2.3. Radius and angular size

We now compute the radius of the ionized region induced by the quasar and first the Strömgren sphere (stationary ionization bounded HII region).

The proper radius R_s of the Strömgren sphere is derived from

$$\frac{4\pi}{3} R_s^3 \alpha_r n_e^2 = S, \quad (5)$$

where n_e is the electronic density $n_e = n_0(1+z)^3$ ($n_0 = 1.13 10^{-5} \Omega_b h^2 \text{ cm}^{-3}$ is the present electronic density). This approximation is valid as long as the photoelectron energy does not exceed the photoionization energy that is to say that a photoelectron is unable to produce additional ionization. The recombination coefficient α_r to all hydrogen levels is given by (Hummer & Seaton 1963)

$$\alpha_r = 1.627 10^{-13} T_4^{-1/2} \times (1 - 1.657 \log T_4 + 0.584 T_4^{1/3}) \text{ cm}^{-3} \text{ s}^{-1}, \quad (6)$$

where T_4 is the temperature of the ionized IGM inside the Strömgren sphere in units of 10^4 K ; thus: $\alpha_r \approx 2 10^{-14} \text{ cm}^3 \text{ s}^{-1}$.

Finally, the Strömgren radius is given by:

$$R_s = \left(\frac{3S}{4\pi\alpha_r n_0^2} \right)^{1/3} (1+z)^{-2}. \quad (7)$$

On the other hand, let us assume that a quasar turns on at a redshift z_{on} and turns off at z_{off} , in the assumption of a lifetime t_q short compared to the expansion time, we have $1+z_{on} \approx 1+z_{off}$. The proper radius R of an ionized bubble that is produced around it at a given time t (when it has not reached the stationary Strömgren sphere state) is computed by writing that every UV photon emitted by the quasar is absorbed through the photoionization of a neutral H atom; therefore the main quantity that rules the size of the bubble is the total number of ionizing photons that are emitted by a quasar during its lifetime: this is given by the product St_q .

The proper radius R will reach a maximum value at the redshift z_{off} (turn off of the quasar) $R_{max}(L_\alpha, z_{off})$; and then it undergoes the average Hubble expansion (the dynamical expansion due to the internal pressure of the bubble can be neglected).

This maximum radius is the solution of:

$$\frac{4\pi}{3} R_{max}^3 n_0 (1+z_{off})^3 = St_q. \quad (8)$$

At a given redshift z smaller than z_{off} , the expansion leads to the radius given by the following relation:

$$R(L_\alpha, z) = \left(\frac{3St_q}{(4\pi)n_0} \right)^{1/3} (1+z)^{-1}, \quad (9)$$

defining $R_c = (3AL_c^* t_q / 4\pi n_0)^{1/3}$ a characteristic radius associated with the characteristic luminosity, L_c^* and the quasar lifetime t_q we finally have:

$$R(l_Q, z) = R_c l_Q^{1/3} (1+z)^{-1}. \quad (10)$$

For $t_q = 10^8 \text{ yrs}$, we find for our choice of cosmological parameters $R_c = 10 \left(\frac{\Omega_b h^2}{0.015} \right)^{-1/3} \left(\frac{\Omega_0}{1} \right)^{-1/6} \text{ Mpc}$.

The comparison of the two computed radii (Eq. (7) and (10)) shows that for redshifts less than z_{eq} where $1+z_{eq} = (t_q \alpha_r n_0)^{-1/3}$, (≈ 47 for $\Omega_b h^2 = 0.0135$ and $t_q = 10^8$ yrs) the ionized bubble is smaller than its Strömgren radius and therefore recombinations can be neglected.

The angular size (radius) of the ionized bubble is $\theta = R/D_A$, where D_A is the angular distance; for a flat universe it is given by

$$D_A = \frac{2c}{H_0} (1+z)^{-2} [1+z - \sqrt{1+z}]. \quad (11)$$

Finally, by defining $\theta_c = R_c H_0 / 2c$, which is given by $\theta_c \approx 3 \left(\frac{\Omega_b h^2}{0.015} \right)^{-1/3} \left(\frac{\Omega_0}{1} \right)^{-1/6} \left(\frac{h}{0.5} \right)$ arcmin, and using Eq. (10) we get

$$\theta = \theta_c l_Q^{1/3} [1 - (1+z)^{-1/2}]^{-1}, \quad (12)$$

which is proportional to $(\Omega_b h^2)^{-1/3} h$, in a flat universe. Figure 1 shows the angular radius of an ionized bubble as a function of redshift for different values of the quasar luminosity and lifetime.

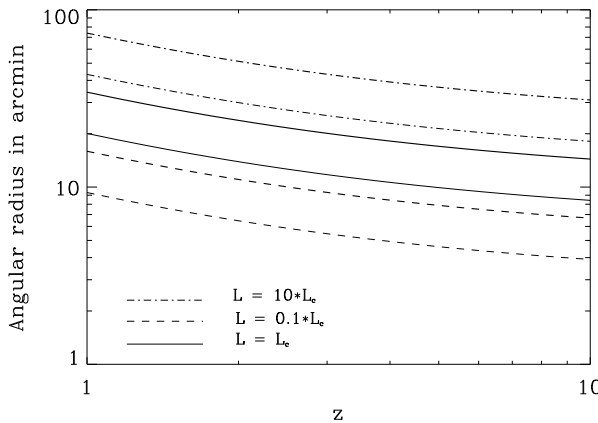


Fig. 1. Angular radius of an ionized bubble as a function of the redshift for three values of the quasar luminosity, where L_c^* is a characteristic luminosity defined Sect. 3.1. The angular radius varies as $L^{1/3}$ see Eq. (12). The series of thin lines stands for the case of the angular radius computed with a quasar lifetime $t_q = 10^7$ yrs, whereas, the thick lines are for $t_q = 5 \cdot 10^7$ yrs. The angular radius increases with $t_q^{1/3}$ (Eq. (12)).

2.4. Optical depth

Knowing the proper radius of the ionized sphere, we can compute the Thomson optical depth for the line of sight going through the center of the bubble:

$$\tau_m = 2 \int_0^R \sigma_T n_e dl, \quad (13)$$

$\sigma_T = 6.65 \cdot 10^{-25} \text{ cm}^2$ is the Thomson cross section. We have thus:

$$\tau_m = 2 \sigma_T n_e(z) R(L_\alpha, z), \quad (14)$$

putting $\tau_c = \sigma_T n_0(z) R_c$ the characteristic optical depth obtained for L_c^* , we have

$$\tau_m = \tau_c l_Q^{1/3} (1+z)^2. \quad (15)$$

The average optical depth over the spherical structure is $\tau_a = \sigma_T n_e(z) \overline{R(L_\alpha, z)}$ with $\overline{R(L_\alpha, z)} = \frac{4}{3} R(L_\alpha, z)$, therefore

$$\tau_a = \frac{2}{3} \tau_m, \quad (16)$$

and it scales like $(\Omega_b h^2)^{2/3} \Omega_0^{-1/6}$. Figure 2 shows the dependence of the bubble optical depth with both the lifetime of the quasar and its luminosity, as a function of the redshift. One should notice in Fig. 2 that the typical optical depth of 10^{-3} (comparable to those of rich clusters) are reached for moderate redshifts.

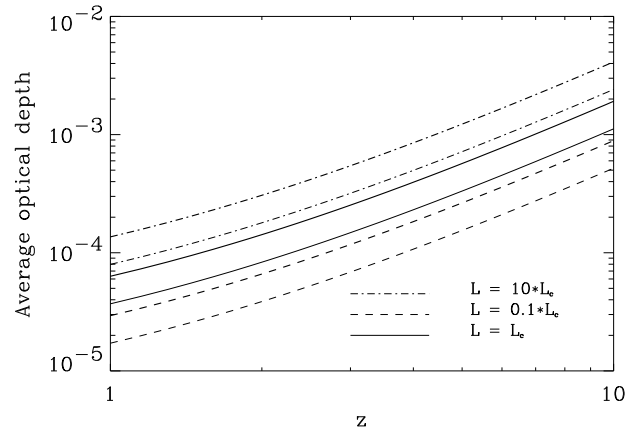


Fig. 2. Average optical depth of an ionized bubble versus redshift for different values of the luminosity with lifetime $t_q = 10^7$ yrs in the case of the thin lines. The thick lines represent the increase due to the increase of the lifetime $t_q = 5 \cdot 10^7$ yrs.

2.5. Thermal Sunyaev-Zeldovich effect

Compton scattering of the CMB radiation on hot free electrons imprints on the incident photon spectrum a signature known as the Sunyaev-Zeldovich thermal effect (SZ) as proposed by Zeldovich & Sunyaev (1969) and Sunyaev & Zeldovich (1972; 1980) by redistributing the photons in the spectrum with a general shift toward higher frequencies. This is an effect that has initially been proposed for clusters of galaxies, and it has already been observed in

the direction of several rich clusters (see for ex Birkingshaw 1990; Birkingshaw et al. 1991; Wilbanks et al. 1994).

The comptonization parameter, y , which characterizes the SZ distortion, depends on the bubble's characteristics and is essentially proportional to the line integral of the electron pressure along the line of sight. For an isothermal sphere, it is given by:

$$y = \frac{k_b T_e}{m_e c^2} \tau; \quad (17)$$

T_e is the electronic temperature and $m_e c^2$ is the electron rest mass. In the Rayleigh Jeans domain the distortion amounts to $\frac{\Delta T}{T} = -2y$. It will be shown to be negligible because of the rather low temperature of the plasma in the bubble.

2.6. Kinetic Sunyaev-Zeldovich effect

Another type of interaction between the bubble and the CMB photons is the SZ kinetic effect (first-order Doppler effect).

The natural reference frame to describe the SZ effect is the local standard of rest defined by the very large scale distribution of matter, i.e the frame in which the CMB is isotropic. If the bubble is at rest in this frame, then the thermal SZ effect (second order effect with respect to the average velocity of the electrons) is the only signature imprinted on the spectrum.

The significance of the so called kinetic effect has been given by Sunyaev & Zeldovich (1972); the motion of a cluster with respect to the background leads (due to the Doppler effect) to an additional change of the radiation temperature in its direction, because of the finite optical depth associated to the bubble. The spectrum of the distortion is indistinguishable from a primordial anisotropy spectrum which is equivalent to a simple temperature change. The observed radiation temperature is changed by $\delta_T = \Delta T/T = -(v_r/c)\tau$, in a direction crossing the bubble where τ is the Thomson optical depth and v_r is the radial component of the bubble peculiar velocity (a positive one corresponds to a recession velocity).

In order to evaluate the relative temperature fluctuations due to the SZ kinetic effect associated with the spheres of plasma around early quasars or left by them after they stop emitting ionizing radiation, we need the optical depth (see Sect. 2.4) and the radial velocity of the bubbles. The average anisotropy associated with an ionized bubble is given by:

$$\delta_T = \frac{2}{3} \frac{v_r}{c} \tau_{cl} l_Q^{1/3} (1+z)^2; \quad (18)$$

this gives us a direct relation between the luminosity of a quasar, its radial velocity, the redshift and δ_T . As regards the cosmological parameters, we have $\delta_T \propto (\Omega_b h^2)^{2/3} \Omega_0^{-1/6}$.

2.7. Velocities

In standard cosmological models, large scale velocities are assumed to be induced by gravity from mass density fluctuations: infall into over dense regions and outfall out of underdense regions. According to the linear gravitational instability theory, the rotational part of the velocity field is diluted by the expansion so that the present large scale cosmic velocity field is expected to be a potential flow. The velocity dispersion of the large scale structures is computed in the assumption of the linear theory; it is given by $\sigma_v(z) = \sigma_{0v}(1+z)^{-1/2}$ (Peebles 1980; 1993), where $\sigma_{0v} = \sigma_v(z=0)$.

In the following, we will assume that the bubbles produced by quasars are random substructures in the linear potential of large scale structures and thus in motion with them. The distribution of their radial velocities is therefore given by the large scale velocity field distribution. The velocities are dominated by the maximum of $\sigma_{0v}(L)$, where L is the corresponding scale, the maximum takes place for scales about 10 Mpc which is still linear at redshifts of interest ($z > 5$). The velocity distribution is directly related to the distribution of primordial density fluctuations during the linear stage; in the assumption of gaussian statistic for the fluctuations, the peculiar one dimensional velocity distribution of the quasars and thus the ionized bubbles is also gaussian, with a velocity dispersion $\sigma_v(z)$.

Numerical simulations have been done to evaluate σ_{0v} and showed for different cosmological models that it was in a range about 700 km/s to 200 km/s depending on the model parameters (Rhee 1993; Croft & Efstathiou 1994).

The observed bulk flow within a sphere out to 6000 km/s is 350 to 400 km/s (Faber et al. 1993). We take here a semi empirical approach using the z dependence given by the linear theory and a conservative value of $\sigma_{0v} = 300$ km/s. The coherence length of the bulk flow could be significantly larger than in the Cold Dark Matter (CDM) model and thus lead to a larger effect.

The ratio of SZ thermal effect to kinetic effect is independent on the optical depth and given by:

$$\frac{k_b T_e}{m_e c^2} \frac{c}{v_r} = 1.7 10^{-2} \left(\frac{T_e}{10^5 \text{ K}} \right) \left(\frac{v_r}{300 \text{ km/s}} \right)^{-1}. \quad (19)$$

Hence the thermal effect is negligible compared with the kinetic effect. This is opposite to what happens for clusters, because the intracluster gas is much hotter ($\approx 10^8$ K).

Figure 3 shows the temperature fluctuation taking for the value of the velocity, the velocity dispersion, as a function of redshift for different luminosities and lifetimes.

3. Quasars distribution

3.1. Quasars luminosity function

The statistics of the measurable bubbles can be deduced if one knows the distribution and evolution of the ionizing sources. This is done when we take into account

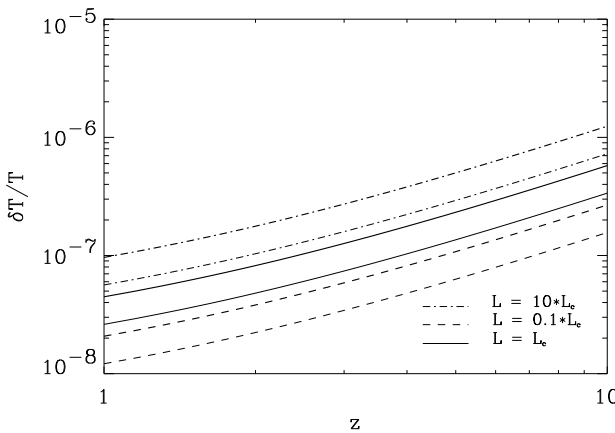


Fig. 3. Temperature fluctuation associated with an ionized bubble versus the redshift for a radial velocity given by the velocity dispersion (Sect. 2.7) and different quasar luminosities. Thin lines are obtained with quasar lifetime $t_q = 10^7$ yrs and thick ones with $t_q = 5 \cdot 10^7$ yrs.

the quasars distribution given by their luminosity function $\Phi(L_\alpha, z)$ which expresses for a given redshift z the comoving space density of quasars as a function of the luminosity.

The quasars luminosity function is not well determined yet, in particular at high redshifts ($z > 3$), owing to the small number of observed sources. Therefore, we will consider different expressions for the luminosity evolution depending on the redshifts range of interest.

According to recent surveys (Boyle, Shanks, & Peterson 1988; Boyle, Jones & Shanks 1991), a pure luminosity evolution model – in which the comoving number density of quasars is assumed to be statistically constant with respect to the time while the luminosity varies with z – describes well the properties of the quasars population up to $z \approx 3$. For $z > 3$, following Warren et al. (1991) and Meiksin & Madau (1993) we introduce a pure density evolution model to describe the population beyond $z \approx 3$ which states that the comoving number density decays exponentially by a factor of 2 per unit redshift (see Hartwick & Shade 1990 for discussion of the quasars luminosity function).

The luminosity function can be written as:

$$\Phi(L_\alpha, z) = \phi(L_\alpha, z)f(z, \tilde{z}), \quad (20)$$

where

$$\phi(L_\alpha, z) = \frac{\Phi^*}{L_\alpha^*(z)} \left\{ \left[\frac{L_\alpha}{L_\alpha^*(z)} \right]^{\beta_1} + \left[\frac{L_\alpha}{L_\alpha^*(z)} \right]^{\beta_2} \right\}^{-1} \quad (21)$$

is the best fit to the quasars luminosity function up to $z \approx 2.9$, (Boyle 1991), and f is a luminosity evolution function (see below).

In a cosmological model with $\Omega_0 = 1$ and $H_0 = 50 \text{ km s}^{-1} \text{ Mpc}^{-1}$, the "best-fit" parameters for the model are (Boyle 1991) $\Phi^* = 6.5 \cdot 10^{-7} \text{ Mpc}^{-3}$, $\beta_1 = 3.9$, $\beta_2 = 1.5$.

The absolute B magnitude, M_B , variation with redshift is expressed by $M_B(z) = M_B^*(z=0) - 2.5k_L \log(1+z)$, where the B magnitude at the present epoch is $M_B^*(z=0) = -22.4$ and $k_L = 3.45$ ("best-fit" parameter). This defines a characteristic luminosity $L_\alpha^*(z) = 10^{-0.4M_B(z)+20.29} \text{ erg s}^{-1} \text{ Hz}^{-1}$.

It finally gives

$$L_\alpha^*(z) = \begin{cases} L_\alpha(0)(1+z)^{k_L} & \text{for } z < z_c \\ L_\alpha^*(z_c) & \text{otherwise,} \end{cases} \quad (22)$$

where z_c is a characteristic redshift, $z_c = 1.9$ ("best-fit" parameter). The luminosity evolution models are expressed by the function $f(z, \tilde{z})$ depending on the value of characteristic redshift \tilde{z} . In the constant comoving range for $z < \tilde{z} = 3$ we have $f(z, \tilde{z}) = 1$, while in the exponential decay mode, for $z > \tilde{z} = 3$, $f(z, \tilde{z}) = \exp(-\mu(z - \tilde{z}))$; μ is the decay constant. The factor 2 decline on the number of the observed quasars at high redshifts gives $\mu = 0.69$.

The comoving spatial density of the quasars in function of the redshift in the range of interest is therefore given by the following expression:

$$\phi(L_\alpha, z) = \frac{\Phi^*}{L_c^*} \exp(-\mu(z-3)) \times \left\{ \left[\frac{L_\alpha}{L_c^*} \right]^{\beta_1} + \left[\frac{L_\alpha}{L_c^*} \right]^{\beta_2} \right\}^{-1} \quad \text{if } z > \tilde{z} = 3. \quad (23)$$

3.2. Quasars formation rate

The luminosity function gives the number of the observed quasars but it can be associated with very different quasars production rate depending on their lifetimes. This is important because we need to include ionized bubbles created by already *dead* quasars. The number of bubbles at a given time is thus larger than the number of radiating sources at the same moment. Only under the assumption that quasars have a lifetime much longer than the age of the universe, does the luminosity function represent the number of ionized spheres. The size of the bubble will increase faster than $(1+z)^{-1}$ if the quasar lifetime is infinite.

A more likely assumption is that the quasar lifetime is short relative to the age of the universe. In this case, although the quasar does not emit any more ionizing photons, it has already produced a long lived bubble that undergoes expansion as we have seen in Sect. 2.3.

We define the rate of production of quasars $Q(L_\alpha, z)$ as

$$Q(L_\alpha, z) = \frac{\Phi(L_\alpha, z)}{t_q}, \quad (24)$$

where we assume that the luminosity function is constant during the short quasar lifetime t_q . This quantity will thus

express the spatial density of ionized bubbles depending on the redshift and the luminosity of the quasars that have formed them.

The theory of quasar formation and evolution is still very uncertain, therefore the quasar lifetime t_q was alternatively given two values $t_q = 10^7$ yrs and $t_q = 10^8$ yrs (Padovani et al. 1990). We note that decreasing the lifetime, leads to the production of smaller and more numerous bubbles.

3.3. Porosity parameter

The Gunn-Peterson (1965) test for hydrogen shows that the universe is ionized at redshift greater than 5. Recent measurements of the Gunn-Peterson effect for helium based upon the Hubble Space Telescope FOC observations by Jakobsen et al. (1994), indicate that the HeII reionization of the universe is partial until $z \approx 3$ (Madau & Meiksin 1994). We suppose that the photoionization of the intergalactic medium is due to the production of HII regions associated with UV sources (quasars); these regions expand and must overlap by $z_{ion} \approx 5$.

In order to evaluate the redshift z_{ion} of the reionization of the universe for hydrogen, one can compute the porosity parameter P . It is the product of the volume associated with an individual ionized bubble by the spatial number density of the bubbles

$$P = \int_z^{+\infty} \frac{dt}{dz_{off}} dz_{off} \int \frac{4\pi}{3} R^3(L_\alpha, z) \phi(L_\alpha, z_{off}) dL_\alpha. \quad (25)$$

Since every UV photon must be absorbed in the IGM, the volume filling factor of ionized hydrogen is equal to the porosity parameter P (and not to $1 - \exp(-P)$), which would be the case if the physics would fix the radius of the bubble rather than the ionized volume). Thus the complete reionization of the IGM occurs for P reaching 1. Figure 4, which is plotted using the set of parameters given in Sect. 1, shows that the assumptions from previous sections lead to $z_{ion} \approx 5.7$. Furthermore, the choice of the cosmological parameters influence the value of the porosity parameter ($P \propto (\Omega_b h^2)^{-1} h^{-1} \Omega_0^{-5/6}$). The reionization redshift is independent on the quasar lifetime as long as the quasars production rate and associated lifetime leads to the observed luminosity function. Our assumptions are therefore compatible with the observed reionization of the universe.

The integration over the luminosity takes into account the total contribution of the quasars to the reionization.

At redshifts where $P \ll 1$, the universe is only partially ionized and the produced ionized bubbles are isolated in a neutral universe. All the quantities defined Sect. 2 (angular size, optical depth and temperature fluctuation) can

thus be computed for these bubbles. Given the luminosity function and the rate of production of quasars we are able to give statistical properties for the relevant quantities; we compute the number of bubbles as a function of the redshift, their angular size and the CMB temperature fluctuation they induce, the surface covering factor...

The induced CMB temperature fluctuations will be dominated by a redshift range in which individual ionized bubbles induce a significant Doppler effect, this is when the hydrogen is still mostly neutral that is for redshifts $z > z_{ion}$.

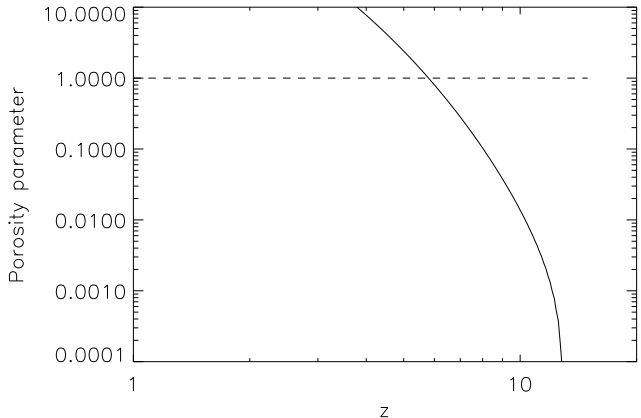


Fig. 4. The porosity parameter is plotted (solid curve) as a function of the redshift. The horizontal dashed line stands for the reionization. Porosity parameter is independent on the lifetime of the quasars.

3.4. Number of bubbles

Starting from the quasars production rate, we first compute the number of ionized bubbles N as a function of their associated temperature fluctuations $\delta_T = \Delta T/T$, their angular sizes θ , redshift z , per units of solid angle. Knowing the number density of bubbles per units of volume, N , which is given by:

$$N = \int_0^t Q(L_\alpha, z) dt. \quad (26)$$

We derive the number of bubbles $dN = NdV$ in the elementary volume $dV = a^3 r^2 dr d\Omega$ with $adr = cdt$ and a the scaling factor $a = (1+z)^{-1}$, $d\Omega$ is the viewing solid angle; with $r = 3ct_0(1 - (1+z)^{-1/2})$ assuming an Euclidean universe.

$$\frac{d^2 N}{dz d\Omega}(L_\alpha, z) = 6 \left(\frac{c}{H_0} \right)^3 \frac{t_0}{t_q} k(z) \times \int_z^{+\infty} \Phi(L_\alpha, z_{off}) (1 + z_{off})^{-5/2} dz_{off}, \quad (27)$$

here $k(z) = (1+z)^{-9/2}[1+(1+z)^{-1/2}]^2$.

Using the quantities computed in Sect. 2 (radius, angular size and optical depth of the ionized bubbles around quasars) which are function of the redshift and the quasar luminosity, we can compute the number of bubbles at redshift z with angular size θ and absolute value of the temperature fluctuation $|\delta_T|$ in the universe, per unit of solid angle as follow:

$$\frac{d^4N}{d\Omega dz d\ln\theta d\ln|\delta_T|} = 2 \times 6 \left(\frac{c}{H_0} \right)^3 \frac{t_0}{t_q} f(z) \theta |\delta_T| \times \int \int \phi(l_Q) g(v_r, z) \delta[l_Q - l_Q(\theta, z)] dl_Q \delta[\delta_T - \delta_T(v_r, l_Q, z)] dv_r \int_z^{+\infty} p(z_{off}) dz_{off}; \quad (28)$$

where δ is the Dirac function, $g(v_r, z)$ is the gaussian distribution for the radial peculiar velocities of the quasars,

$$f(z) = (1+z)^{-9/2}[1+(1+z)^{-1/2}],$$

$$p(z_{off}) = (1+z_{off})^{1/2} \exp[-0.69(z_{off}-3)]$$

and $l_Q(\theta, z)$ is derived from Eq. (12) and v_r from Eq. (18).

There are as many negative sources as positive ones, therefore the factor 2 is introduced when we take into account the negative and positive radial velocities of the bubbles and give the counts as a function of $|\delta_T|$. We note that in a flat universe, the number of bubbles scales like $(\Omega_b h^2)^{1/3} h^{-3}$.

The results have been numerically computed and are plotted Fig. 5 and Fig. 6, integrated over the redshifts ($z > 6$) for different values of quasar lifetime ($t_q = 10^8$ yrs and $t_q = 10^7$ yrs).

Next, we also compute the covering surface parameter C_S which is the fraction of the sky covered by ionized bubbles inducing a distortion of amplitude δ_T and angular size θ at redshift z . This is done by multiplying the previous counts by the solid angle occupied by the bubbles; we obtain:

$$C_S = 2 \times 6 \left(\frac{c}{H_0} \right)^3 \frac{t_0}{t_q} f(z) \times \int \int \pi \theta^2 \phi(l_Q) g(v_r, z) dl_Q dv_r \delta[l_Q - l_Q(\theta, z)] \delta[\delta_T - \delta_T(v_r, l_Q, z)] \int_z^{+\infty} l(z_{off}) dz_{off}. \quad (29)$$

Factor 2 takes into account the sources with both negative and positive velocities, and $C_S \propto (\Omega_b h^2)^{-2/3} h^{-2}$ for a flat universe.

The results plotted Fig. 7 and Fig. 8 are also integrated over z and given for the two previous values of the quasar lifetime t_q .

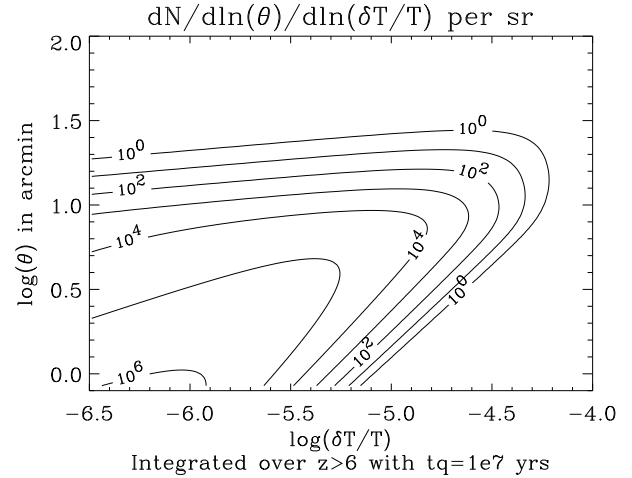


Fig. 5. The number of ionized bubbles per unit solid angle, logarithmic interval of $|\delta_T|$ logarithmic interval of the angular radius θ is plotted as a function of the temperature fluctuation $\log\delta_T$ and $\log\theta$ in arcmin. This number is integrated over the redshifts ($z > 6$) and computed for lifetime $t_q = 10^7$ yrs according to Eq. (28).

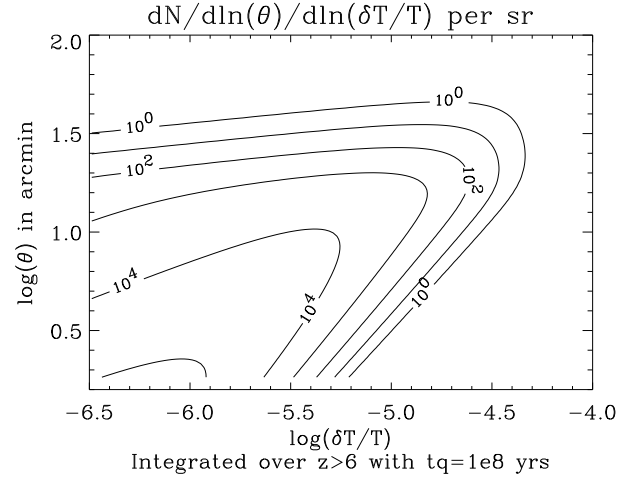


Fig. 6. The same quantity is plotted for a quasar lifetime $t_q = 10^8$ yrs. The bubbles are greater but less numerous.

3.5. Anisotropies during fully ionized period

When the IGM is totally ionized at $z < z_{ion} = 5.7$, we evaluate the rms temperature fluctuation. The optical depth is almost constant in this redshift range ($z < z_{ion}$) whereas the velocities are variable. Therefore, we compute the average of the temperature fluctuation along a line of sight

$$\delta_T = \sigma_T \int_0^{t_0} n_e v_r dt. \quad (30)$$

The fluctuation is due to the peculiar velocity variation which is expressed by the velocity dispersion. In the linear perturbation theory, it is shown that the velocities de-

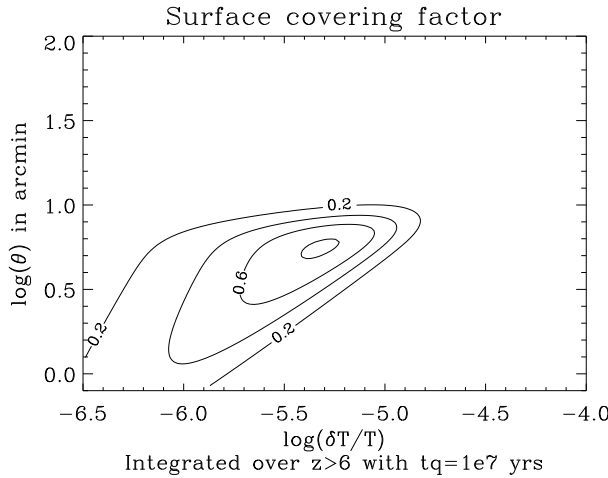


Fig. 7. The surface covering factor of the ionized bubbles per logarithmic interval of $|\delta_T|$ and logarithmic interval of the angular radius θ is plotted as a function of the temperature fluctuation ($\log \delta_T$) and $\log \theta$ in arcmin. It is integrated over the redshifts ($z > 6$) and computed for lifetime $t_q = 10^7$ yrs according to Eq. (29)

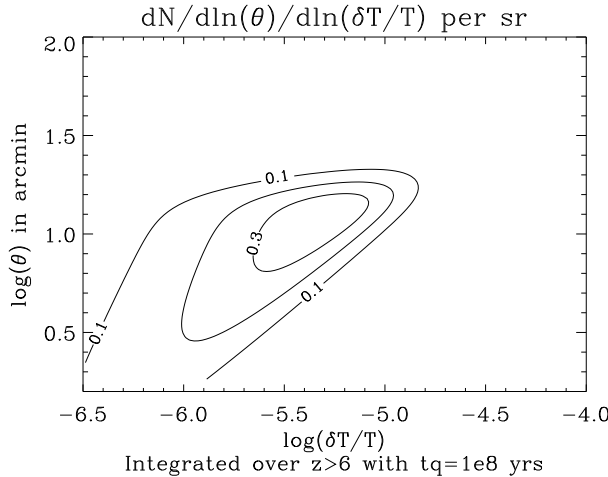


Fig. 8. The surface covering factor is plotted for quasar lifetime $t_q = 10^8$ yrs

pend upon the scales of the density perturbation that are associated with them and it is also shown that in a CDM model the coherence length is short. Other cosmological models could give a stronger effect.

Using the velocity dispersion of the distribution, we compute the rms temperature fluctuation $(\delta_T)_{rms}$ when the IGM is fully ionized, and find

$$(\delta_T)_{rms} \approx 1.5 \cdot 10^{-6} \left(\frac{\Omega_b h^2}{0.015} \right) \left(\frac{h}{0.5} \right)^{-1}. \quad (31)$$

We note that the effect due to the velocity variation is one order of magnitude lower than the rms fluctuation detected by COBE (Mather et al. 1994) and it is at the

limit sensitivity of the modern detectors, the average effect of velocity field in the fully ionized universe is therefore weaker than the effect for a partially ionized universe.

4. Discussion

We discuss here the effects of ionization of the IGM by early formed quasars on the cosmic microwave background as calculated in previous sections.

We have shown the thermal SZ effect was negligible compared to the kinetic one. The amplitude of the largest temperature fluctuations induced by the latter mechanism are comparable to the the primordial fluctuations at scales comparable with the scales of the Doppler peaks ($10'$ to 1°). These secondary fluctuations have no spectral signature to distinguish them from the primordial ones. Hence, future observations and detections of the CMB at small scales with sensitivity about 10^{-6} will have to take into account the possible presence of such objects in the sky.

When the porosity parameter is lower than 1 for $z > z_{ion}$, we have computed the number of ionized bubbles per unit of solid angle, with respect to their angular radius and to δ_T the temperature fluctuation they induce integrating over the redshifts.

We plot (Fig. 6) the number of kinetic effect sources integrated over redshifts ($z > 6$) per unit solid angle, first for lifetime $t_q = 10^8$ yrs. We find that there are approximately 10^4 objects per unit solid angle with associated temperature fluctuations some 10^{-6} and angular radius 3 to 10 arcmin randomly distributed over the sky and about 10 ionized bubbles per unit solid angle with temperature fluctuations with about $3 \cdot 10^{-5}$ and radius about 12 to 30 arcmin. With the same set of parameters, we plot (Fig. 8) the surface covering factor integrated over redshifts versus the amplitude of the anisotropies and their angular radius.

The counts depend significantly on the quasar lifetime value, in fact, it was shown that decreasing the lifetime t_q decreases the size of the bubbles, but on the other hand, it increases the rate of formation of quasars and thus gives more numerous bubbles. Figures 5 and 7 show respectively the number of bubbles per unit solid angle and covering surface versus δ_T and the angular radius for $t_q = 10^7$ yrs. In this configuration, we find that there are 100 objects per steradian with δ_T about 10^{-5} and radius 5 to 12 arcmin.

Therefore, early quasars will induce distortions with different statistical properties than the primordial ones and produce rare fluctuations with amplitude of up to 10^{-5} . Although the rms value of the fluctuations induced by the inhomogeneous reionization is smaller, by an order of magnitude, than the rms of the fluctuations detected by COBE (COsmic Background Explorer) (Smoot et al. 1992; Mather et al. 1994), the largest ones at small angular scales could be dominated by the effect discussed here. Hence high accuracy measurements of the power spectrum of the CMB anisotropies such as those considered for future space experiments (better than 1%) and search for

deviations to Gaussian statistics must take into account this kind of sources. We find that most of the anisotropies with high level $\Delta T/T$ and small angular scales are given by quasars at high redshifts.

Observations from the first flight of the Medium Scale Anisotropy Measurement (MSAM) (Cheng et al. 1994) with a $30'$ beam instrument, showed the presence of two unresolved sources from a survey of $7.6 \cdot 10^{-3}$ sr with $\delta_T \approx 3 \cdot 10^{-5}$ consistent spectrally with CMB anisotropies ; this implies about 200 of such sources per steradian.

The temperature fluctuations produced by the effect that we are studying – ionization by early quasars – are indistinguishable from primordial anisotropies. Furthermore, the computations done for our model with short quasar lifetime $t_q = 10^7$ yrs predicts about 100 events per unit solid angle with angular diameter about $20'$ and $\delta_T \approx 3 \cdot 10^{-5}$, consistent with the results of the MSAM observations. In this context, the statistics of such events on the sky will be an important criterion to attribute an origin to them.

Figure 7 – representing the surface covering factor – shows that the ionized bubbles around quasars are close to cover the whole sky although they do not fill the space until $z < z_{ion} = 5.7$. Therefore, we can no longer consider the induced temperature fluctuations as individual sources. On the contrary, it is necessary to get statistical informations about the distribution of the anisotropies such as the standard deviation, mean value, kurtosis... Hence we have simulated maps of the anisotropies induced by the quasars.

The maps were drawn under simple geometrical assumptions (spherical bubbles), using the counts of ionized bubbles associated with quasars characterized by an angular radius and a temperature fluctuation given in Eq. (28) and using the fact that there is a simple relation between the angular radius of the bubble and the luminosity of the quasar that induced it, Eq. (12). We put a limit on the number of bubbles; for numbers of bubbles greater than this limit, a gaussian drawing is done otherwise we make a poissonian drawing. The positions of the bubbles over the map are random, this is a rather good assumption since the clustering of quasars is still uncertain.

We check that the standard deviation, mean, maximum and minimum values are found consistent with the bubbles counts. But as could be expected, the distribution of the temperature fluctuations induced by quasars is far from being gaussian. Indeed, for a typical value of the quasar lifetime $t_q = 10^7$ yrs we find that the kurtosis is equal to 1.4. This is an important result that might be taken into account if one wants to test the gaussianity of the primordial anisotropies of the CMB, to prove whether or not the primordial fluctuations are adiabatic (thus due to quantum fluctuations of the vacuum energy) for which the statistic is gaussian or to topological defaults (strings, domain walls, ...). In fact, the presence of

early ionizing sources (quasars here) induces additional non gaussian anisotropies with no spectral signature.

Cosmological models show that there is an angular cut off in the spectrum of the primordial anisotropies. The bubbles contribution to the observed CMB at small angular scales could be important or may be dominant, in particular at scales where the primordial fluctuations are "washed out" because of the damping associated with the width of the the last scattering surface. This effect is suggested Fig. 9, where we plot both the power spectra of the primordial temperature fluctuations and the bubbles in terms of the spherical harmonics coefficients (see for example White, Scott & Silk 1994); taking $t_q = 10^7$ yrs. Our results show that the secondary anisotropies of the

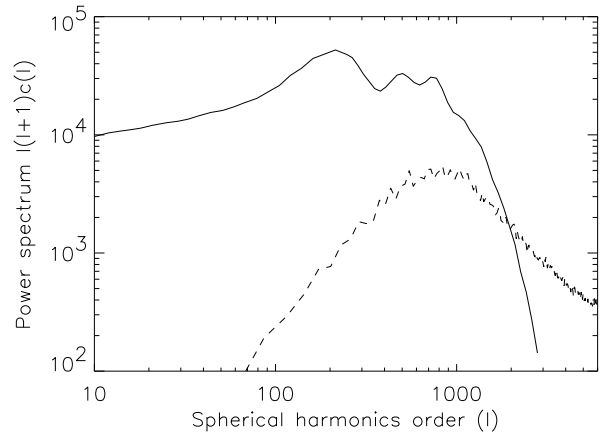


Fig. 9. Power of the anisotropies induced by the bubbles and the primordial fluctuations in the spherical harmonics versus the multipoles. *Solid curve* for the primary CMB and *dashed curve* for the fluctuations induced by the quasars we take $t_q = 10^7$ yrs

CMB, produced by the kinetic SZ effect in ionized bubbles around quasars, must be taken into account.

In the future, observations along the lines of sight of known quasars at high redshift showing the Gunn-Peterson effect, could be an interesting test to detect this kinetic effect induced by the ionized bubbles. The following calculations are possible only for the bubbles associated with the strongest temperature fluctuations for which primordial anisotropies do not perturb too much the observations. In that case, we could be able to derive the bubble peculiar velocity.

In Sect. 2.6, We have derived a simple relation between the temperature fluctuation associated with an ionized bubble, the radial peculiar velocity and the luminosity of the quasar that has produced it Eq. (18). On the other hand, Eq. (12) gives the the expression of the angular radius of the the bubble as a function of the quasar luminosity. Therefore, if we observe a bubble inducing a

temperature fluctuation, we directly derive the luminosity from the angular size and knowing this we have a direct measure of the peculiar radial velocity. The latter is given by the following expression

$$\frac{v_r}{c} = \frac{3}{2} \frac{\delta_T}{\theta} \frac{\theta_c}{\tau_c} (1+z)^{-2} [1 - (1+z)^{1/2}]^{-1}, \quad (32)$$

where θ_c and τ_c are defined respectively in Sect. 2.3. and Sect. 2.4.

In the hypothesis of an ionization due to individual sources of radiation, the whole formalism we develop remains valid whatever the kind of sources, early galaxies, first generation of stars, ... The effect of the presence of sources of luminosity of the same order as the quasars on the CMB will be the same as the one described for quasars.

Acknowledgements. The authors thank M. Lachièze-Rey and F. R. Bouchet for helpful discussions, and an anonymous referee for helpful comments.

References

Bechtold, J. 1994, *ApJS*, **91**, 1

Bechtold, J. et al. 1987, *ApJ*, **315**, 180

Birkinshaw, M. 1990, in *The cosmic microwave background: 25 Year Later*, eds. N. Mandolesi and N. Vittorio (Kluwer: Dordrecht)

Birkinshaw, M., Hughes, J. P., & Arnaud, K. A. 1991, *ApJ*, **379**, 466

Blanchard, A. 1991, in *The infrared and Submillimetre Sky after COBE*, NATO ASI series edited by Signore, M. & Dupraz, C.

Bond, J. R., & Efstathiou, G. 1984, *ApJ*, **285**, L45

Boyle, B. J. 1991, in Texas/ESO-CERN Symposium on Relativistic Astrophysics, Cosmology and Fundamental Physics

Boyle, B. J., Shanks, T., & Peterson, B. A. 1988, *M.N.R.A.S.*, **235**, 935

Boyle, B. J., Jones, E. R., & Shanks, T. 1991, *M.N.R.A.S.*, **251**, 482

Cheng, E. S., Cottingham, D. A., Fixsen, D. J., Inman, C. A., Kowitt, M. S., Meyer, S. S., Page, L. A., Puchalla, J. L., Silverberg, R. F. 1994, *ApJ*, **422**, L37

Couchman, h. M. P. & Rees, M. J. 1986, *M.N.R.A.S.*, **221**, 53

Cox, D., P., & Smith, B., W., 1974, *ApJ*, **189**, L105

Croft, R. A. C., & Efstathiou, G. 1994, *M.N.R.A.S.*, **268**, L23

Dalgarno, A., & McCray, R. A. 1972, *ARA&A*, **10**, 375

Donahue, M. J. & Shull J. M. 1987, *ApJ*, **323**, L13

Faber, S. M., Courteau, S. J. A., Yahil, A. 1993, in Proc. 9th IAP Astrophysics Meeting, *Cosmic Velocity Fields*, ed. M. Lachièze-Rey & F. R. Bouchet (Editions Frontières)

Gundersen, J. O., Clapp, A. C., Delvin, M., Holmes, W., Fisher, M. L., Meinhold, P. R., Lange, A. E., Lubin, P. M., Richards, P. L., Smoot, G. F. 1993, *ApJ*, **413**, L1

Gunn, J. E., & Peterson, B. A. 1965, *ApJ*, **142**, 1633

Hartwick, F. D. A., & Shade, D. 1990, *ARA&A*, **28**, 437

Hummer, D. G., & Seaton, M. J. 1963, *M.N.R.A.S.*, **125**, 437

Ikeuchi, S. 1981, *Pub. Astr. Soc. Japan*, **33**, 211

Jakobsen, P., Boksenberg, A., Deharveng, J. M., Greenfield, P., Jedrzejewski, R., & Paresce, F. 1994, *Nature*, in press

Katz, N., Quinn, T., Bertschinger, E., & Gelb, J. M. 1994, *M.N.R.A.S.*, **270**, L71

Madau, P., & Meiksin, A. 1994, to be published in *ApJ letters*

Meiksin, A., & Madau, A. 1993, *ApJ*, **412**, 34

Mather, J. C. et al. 1994, *ApJ*, **420**, 439

Miralda-Escudé, J. & Ostriker, J. P. 1990, *ApJ*, **350**, 1

Miralda-Escudé, J. & Ostriker, J. P. 1992, *ApJ*, **392**, 15

O'Brien, P. T. et al. 1988, *M.N.R.A.S.*, **233**, 801

Padovani, P., Burg, R., & Edelson, R. A. 1990, *ApJ*, **353**, 438

Peebles, P. J. E. 1980, in *The Large Scale Structure of the Universe*, Princeton University Press

Peebles, P. J. E. 1993, in *Principles of Physical Cosmology*, Princeton University Press

Rhee, G., 1993, *ApJ*, **411**, 455

Smoot, G. F., et al. 1992, *ApJ*, **396**, L1

Sunyaev R. A., & Zeldovich, Ya. B. 1980, *M.N.R.A.S.*, **190**, 413

Tegmark, M., & Silk, J. 1994, *ApJ*, **423**, 529

Tegmark, M., Silk, J., & Blanchard, A. 1994, *ApJ*, **420**, 484

Vishniac, E. T. 1987, *ApJ*, **322**, 597

Vishniac, E. T. & Ostriker, J. P. 1985, in Proc. 3rd Rome Meeting on Astrophysics, *The Cosmic Background Radiation and Fundamental Physics*, ed. F. Melchiorri (Bologna:Italian Physical Society)

Vittorio, N., & Silk, J. 1984, *ApJ*, 285, L39

Voit, G. M. 1994, *ApJ*, L19

Walker et al. 1991, *ApJ*, **376**, 51

Warren, S. J., Hewett, P. C., & Osmer, P. S. 1991, in *The Space Distribution of Quasars*, ed. D. Crampton (ASP Conf. Ser 21), 139

White, M., Scott, D. & Silk, J. 1994, *ARA&A*, **32**, 319

Wilbanks, T. M., Ade, P. A. R., Fisher, M. L., Holzapfel, W. L., Lange, A. E. 1994, *ApJ*, **427**, L75

Zuo, L., & Phinney, E. S. 1993, *ApJ*, **418**, 28